

# Estimation of Extended Targets Based on Compressed Sensing in Cognitive Radar System

Peng Chen, *Student Member, IEEE*, Chenhao Qi, *Senior Member, IEEE*,  
Lenan Wu, and Xianbin Wang, *Senior Member, IEEE*

**Abstract**—In this paper, the ranges and velocities of multiple extended targets are estimated by exploiting the target sparsity in the cognitive radar system. Different from the point targets in the traditional compressed sensing (CS) radar, the parameters of extended targets are expressed and estimated by using a novel CS-based model. Since the echo signals from extended targets are the convolutions between the transmitted waveform and target impulse responses (TIRs), the dictionary matrices in the proposed cognitive radar for all extended targets must be first established in the CS-based reconstruction algorithm. Then, the target parameters are estimated by reconstructing the nonzero entries of a sparse vector. To further improve the performance of CS reconstruction, a novel two-step method is proposed to minimize the mutual coherence of the dictionary matrix by optimizing the transmitted waveform. Simulation results demonstrate that the estimation performance of the extended targets is significantly improved by optimizing the transmitted waveform.

**Index Terms**—Compressed sensing (CS)-based radar system, delay-Doppler plane, multiple extended targets, waveform optimization.

## I. INTRODUCTION

THE compressed sensing (CS) theory has been widely applied in many different fields, including radar systems, wireless communications, and image processing [1], [2]. With the CS theory, a sparse signal can be reconstructed from far fewer measurements than that required in traditional sampling theory [3]–[6]. The relative Doppler shifts and delays between the transmitted and received echoes are commonly adopted to measure the target velocities and ranges in radar systems, which can be represented by the corresponding points in a

Manuscript received March 14, 2016; accepted May 4, 2016. Date of publication May 10, 2016; date of current version February 10, 2017. This work was supported in part by the National Natural Science Foundation of China under Grant 61302097, Grant 61271204, and Grant 61174205, and in part by the Ph.D. Programs Foundation of the Ministry of Education of China under Grant 20120092120014. The review of this paper was coordinated by Prof. W. A. Hamouda. (*Corresponding author: Chenhao Qi.*)

P. Chen is with the School of Information Science and Engineering, Southeast University, Nanjing 210096, China, and also with the Department of Electrical Engineering, Columbia University, New York, NY 10027 USA (e-mail: chenpengdsp@seu.edu.cn).

C. Qi and L. Wu are with the School of Information Science and Engineering, Southeast University, Nanjing 210096, China (e-mail: qch@seu.edu.cn; wuln@seu.edu.cn).

X. Wang is with the Department of Electrical and Computer Engineering, University of Western Ontario, London, ON N6A 3K7, Canada (e-mail: xianbin.wang@uwo.ca).

Color versions of one or more of the figures in this paper are available online at <http://ieeexplore.ieee.org>.

Digital Object Identifier 10.1109/TVT.2016.2565518

delay-Doppler plane. Therefore, by exploiting the target sparsity in this plane, the CS-based reconstruction algorithms are adopted to estimate these target parameters [7].

In the CS radar with point targets, the same estimation performance can be achieved by far fewer measurements than that required in the traditional radars [8]. For example, the CS-based multiple-input-multiple-output (MIMO) radar is proposed in [9], where the high-resolution estimations about the target range, angle, and velocity are achieved by a narrow-band step frequency waveform. However, the CS-based method has not been proposed to estimate the ranges and velocities of multiple extended targets. Therefore, in this paper, we propose a novel CS-based radar system to exploit the sparsity of extended targets in the delay-Doppler plane.

On the other hand, cognitive radar as the future trend of the radar system has been widely investigated in recent years due to its improved performance and adaptability in different operation environment [10]–[12]. Generally, there are three critical elements in the cognitive radars [10]:

- 1) the intelligent signal processing based on the radar operation environment;
- 2) the feedback between the receiver and transmitter;
- 3) the preservation information in echo waveform.

To further improve the estimation, detection, and tracking performances of cognitive radar, the transmitted waveform is optimized according to the radar working environment [13]–[16]. In the existing studies, waveform optimization is mainly focused on maximizing the following two metrics [17]–[22]:

- 1) the mutual information between the echo waveform and extended target;
- 2) the signal-to-interference-and-noise ratio (SINR) of echo waveform.

However, it remains challenging to design CS-based cognitive radar system particularly for the detection of multiple targets. Both the optimization methods and objective functions in the CS radar are different from those in the traditional radars. Furthermore, both transmitted waveform and sensing matrix can be optimized to further improve the reconstruction performance of the CS radar [23] in achieving the cognitive operational capability. In most cases, the sensing matrix follows the sub-Gaussian distribution, resulting in a high probability that satisfy the restricted isometry property (RIP) [3]. Thus, the waveform optimization has been the primary method to improve the CS-based reconstruction performance, which is measured by the RIP of the dictionary matrix. However, in the cognitive radar,

the method to improve the performance of CS reconstruction by optimizing the transmitted waveform for multiple extended targets has yet to be proposed.

It has been shown that obtaining the RIP is a nondeterministic polynomial-time (NP)-hard problem, and mutual coherence is proposed as an alternative of RIP [24]. To minimize the mutual coherence of the dictionary matrix for point targets, several methods have been proposed by optimizing the transmitted waveform [25]. For example, in [26], the power among antennas to improve the target position and velocity estimation performance is optimized; in [27], better target localization performance in the angle–Doppler–range space is achieved by minimizing the mutual coherence and improving the signal-to-interference ratio. However, for extended targets, neither the CS-based model nor the waveform optimization method has been proposed.

In this paper, we investigate the range and velocity estimation problem for multiple extended targets and propose a CS-based radar model to exploit the sparsity of extended targets in the delay–Doppler plane. Different from traditional CS radar of which the dictionary matrix only contains the delays and Doppler shifts of the originally transmitted waveform, the proposed CS radar adopts novel dictionary matrices for multiple extended targets. Additionally, the sparse vector is reconstructed by the CS-based method, where the nonzero entries indicate the corresponding target parameters. To minimize the mutual coherence of the dictionary matrix, we also propose a novel two-step method for optimizing the transmitted waveform. In the first step, the waveforms are individually optimized for each extended target through an iterative algorithm. In the second step, the weight vector is optimized to combine the output waveforms in the first step.

The organization of this paper is as follows. In Section II, the radar system with multiple extended targets is described, and a novel CS-based system model is formulated in the delay–Doppler plane. In Section III, a novel method of waveform optimization is proposed to minimize the mutual coherence of the dictionary matrix. Simulation results are given in Section IV, and Section V discusses the relationship between the number of targets and that of measurements. Section VI concludes this paper.

The notations used in this paper are defined as follows. Symbols for vectors (lower case) and matrices (upper case) are in boldface.  $\mathbf{I}_N$ ,  $\mathcal{CN}(0, \mathbf{R})$ ,  $(\cdot)^T$ ,  $(\cdot)^H$ ,  $\text{diag}\{\cdot\}$ ,  $*$ ,  $\lfloor \cdot \rfloor$ , and  $\|\cdot\|_2$  denote the  $N \times N$  identity matrices, the complex Gaussian distribution with zero mean and covariance being  $\mathbf{R}$ , the transpose, the conjugate transpose (Hermitian), the diagonal matrix, the convolution, the floor function, and the  $\ell_2$  norm, respectively.

## II. RADAR SYSTEM MODEL WITH MULTIPLE EXTENDED TARGETS

### A. Received Signal

In [7] and [28], the CS-based model has been studied to describe the point targets, where the echo waveforms from targets are the delays or Doppler shifts of the originally transmitted waveform. However, when targets are large enough to

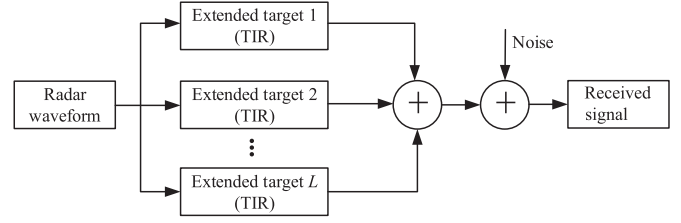


Fig. 1. Radar system model with extended targets.

occupy more than one resolution cell, it is more appropriate to be described by extended targets [29]. As shown in Fig. 1, there are  $L$  extended targets that are described by the target impulse responses (TIRs) [10]–[14]. For the  $l$ th extended target, the velocity, range, and TIR are denoted by  $v_l$ ,  $D_l$ , and  $h_l(t)$ , respectively. Then, the echo waveform from the  $l$ th target can be obtained as

$$g_l(\tau_l, f_{D,l}, t) = h_l(t - \tau_l) * s(t - \tau_l) e^{j2\pi f_{D,l} t} \quad (1)$$

where  $*$  denotes the convolution operation,  $s(t)$  ( $t \in [0, T)$ ) denotes the transmitted waveform,  $t$  denotes the continuous time,  $T$  denotes the pulse duration,  $\tau_l = 2D_l/c$  denotes the delay,  $f_{D,l} = (2v_l/c)f_C$  denotes the Doppler frequency caused by target movement,  $f_C$  denotes the carrier frequency, and  $c$  denotes the waveform speed. Therefore, the received signal can be expressed as the superposition of the echo waveforms from all targets

$$r(t) = \sum_{l=0}^{L-1} g_l(\tau_l, f_{D,l}, t) + n(t) \quad (2)$$

where  $n(t)$  denotes the additive white Gaussian noise (AWGN).

For simplicity, the continue time signal  $r(t)$  is expressed in the form of discrete vector. Since both delay and Doppler shift are contained in  $r(t)$ , the received signal is simplified by the following two steps.

- 1) *Delay*: With only delay  $\tau_l$ , the waveform  $g_l(\tau_l, 0, t)$  is sampled with sampling frequency  $f_S$  and can be expressed in a vector form as follows:

$$\mathbf{g}_l(\tau_l, 0) = \left[ \mathbf{0}_{N_{\tau_l}}, \mathbf{g}_l^T, \mathbf{0}_{N_R - N_{\tau_l} - N} \right]^T \quad (3)$$

where  $\mathbf{g}_l \triangleq \mathbf{g}_l(0, 0)$  denotes the vector form of  $g_l(0, 0, t)$  with the length being  $N = \lfloor T f_S \rfloor$ ,  $\mathbf{0}_{N_{\tau_l}}$  denotes a zero vector with the length being  $N_{\tau_l} = \lfloor \tau_l f_S \rfloor$ , and  $N_R$  denotes the length of  $\mathbf{g}(D_l, 0)$ .

- 2) *Doppler frequency*: With only Doppler frequency  $f_{D,l}$ , the waveform  $g_l(0, v_l, t)$  is sampled with the sampling frequency being  $f_S$  and can be expressed in a vector form as

$$\mathbf{g}_l(0, f_{D,l}) = \mathbf{E}_N(f_{D,l}) \mathbf{g}_l \quad (4)$$

where the diagonal matrix  $\mathbf{E}_N(f_{D,l}) \in \mathbb{C}^{N \times N}$  is defined as

$$\mathbf{E}_N(f_{D,l}) \triangleq \text{diag} \left\{ e^{j2\pi \frac{f_{D,l}}{f_S}}, e^{j2\pi \frac{2f_{D,l}}{f_S}}, \dots, e^{j2\pi \frac{Nf_{D,l}}{f_S}} \right\}. \quad (5)$$

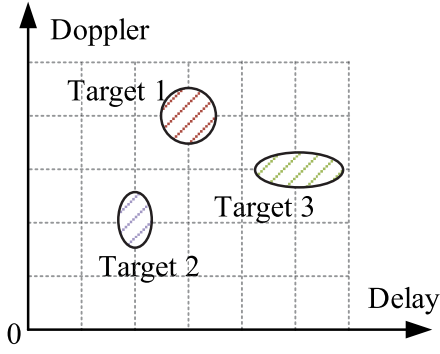


Fig. 2. Multiple extended targets in the delay–Doppler plane.

Denoting  $\mathbf{h}_l \in \mathbb{C}^{N \times 1}$  as the vector form of  $h_l(t)$ , a convolution matrix can be expressed as

$$\mathbf{H}_l \triangleq \begin{pmatrix} h_l(0) & h_l(N-1) & \dots & h_l(1) \\ h_l(1) & h_l(0) & \dots & h_l(2) \\ \vdots & \vdots & \ddots & \vdots \\ h_l(N-2) & h_l(N-3) & \dots & h_l(N-1) \\ h_l(N-1) & h_l(N-2) & \dots & h_l(0) \end{pmatrix} \quad (6)$$

where  $h_l(i)$  ( $i = 0, 2, \dots, N-1$ ) is the  $i$ th entry of  $\mathbf{h}_l$ . Therefore, with both delay and Doppler frequency, the waveform  $g(\tau_l, f_{D,l}, t)$  can be expressed in the vector form as

$$\begin{aligned} g_l(\tau_l, f_{D,l}) &= \mathbf{E}_{N_R}(f_{D,l}) \mathbf{g}_l(D_l, 0) \\ &= \mathbf{M}(f_{D,l}) \mathbf{D}(\tau_l) \mathbf{H}_l \mathbf{s} \end{aligned} \quad (7)$$

where  $\mathbf{D}(\tau_l) \triangleq [\mathbf{0}_{N_{\tau_l} \times N}^T, \mathbf{I}_N, \mathbf{0}_{(N_R - N - N_{\tau_l}) \times N}^T]^T$ ,  $\mathbf{0}_{N_{\tau_l} \times N}$  denotes an  $N_{\tau_l} \times N$  matrix with all entries being zeros,  $\mathbf{s} \in \mathbb{C}^{N \times 1}$  denotes the vector form of  $s(t)$ , and  $\mathbf{M}(f_{D,l}) \triangleq \mathbf{E}_{N_R}(f_{D,l})$ .

Finally, the vector form of the received signal in (2) can be obtained as follows:

$$\mathbf{r} = \sum_{l=1}^L \mathbf{g}_l(\tau_l, f_{D,l}) + \mathbf{n} \quad (8)$$

where  $\mathbf{n} \sim \mathcal{CN}(\mathbf{0}, \sigma_n^2 \mathbf{I}_{N_R})$  denotes the AWGN noise.

### B. CS-Based System Model

As shown in Fig. 2, the  $l$ th extended target with delay  $\tau_l$  and Doppler frequency  $f_{D,l}$  corresponds to a point in the delay–Doppler plane. Since the targets are sparse in the discretized delay–Doppler plane, a novel CS-based model is proposed here to describe the extended targets. Denote  $P$  and  $Q$  as the number of delay and Doppler frequency bins, respectively. The delay and Doppler frequency are respectively discretized into  $(0, 1, \dots, P-1)\Delta\tau$  and  $(0, 1, \dots, Q-1)\Delta f_D$ , where  $\Delta\tau$  and  $\Delta f_D$  are the delay and Doppler frequency resolutions, respectively. Then, the overcomplete dictionary matrix for each extended target can be established by collecting all the echo waveforms with different

delays and Doppler frequencies. For the  $l$ th extended target, the dictionary matrix can be expressed as

$$\begin{aligned} \mathbf{A}_l &\triangleq \begin{bmatrix} \mathbf{g}_l^T(0 \cdot \Delta\tau, 0 \cdot \Delta f_D) \\ \mathbf{g}_l^T(0 \cdot \Delta\tau, 1 \cdot \Delta f_D) \\ \vdots \\ \mathbf{g}_l^T(0 \cdot \Delta\tau, (Q-1) \cdot \Delta f_D) \\ \vdots \\ \mathbf{g}_l^T(1 \cdot \Delta\tau, 1 \cdot \Delta f_D) \\ \vdots \\ \mathbf{g}_l^T((P-1) \cdot \Delta\tau, (Q-1) \cdot \Delta f_D) \end{bmatrix}^T \\ &= \mathbf{K}^T [\mathbf{I}_{PQ} \otimes (\mathbf{H}_l \mathbf{s})^T]^T \end{aligned} \quad (9)$$

where  $\otimes$  denotes the Kronecker product, and

$$\mathbf{K} \triangleq \begin{bmatrix} \mathbf{D}^T(0 \cdot \Delta\tau) \mathbf{M}^T(0 \cdot \Delta f_D) \\ \mathbf{D}^T(0 \cdot \Delta\tau) \mathbf{M}^T(1 \cdot \Delta f_D) \\ \vdots \\ \mathbf{D}^T(0 \cdot \Delta\tau) \mathbf{M}^T((Q-1) \cdot \Delta f_D) \\ \vdots \\ \mathbf{D}^T(1 \cdot \Delta\tau) \mathbf{M}^T((Q-1) \cdot \Delta f_D) \\ \vdots \\ \mathbf{D}^T((P-1) \cdot \Delta\tau) \mathbf{M}^T((Q-1) \cdot \Delta f_D) \end{bmatrix} \quad (10)$$

Thus, the echo waveform in (7) can be rewritten as

$$\mathbf{g}_l(\tau_l, f_{D,l}) = \mathbf{A}_l \mathbf{x}_l \quad (11)$$

where  $\mathbf{x}_l$  denotes a sparse vector with length being  $P \times Q$ . Note that the nonzero entries of  $\mathbf{x}_l$  represent the scattering coefficients, and the index of the nonzero entry corresponds to a pair of target delay and Doppler frequency.

Collecting the dictionary matrices for all extended targets, the following dictionary matrix can be obtained as follows:

$$\begin{aligned} \mathbf{A} &\triangleq [\mathbf{A}_1, \mathbf{A}_2, \dots, \mathbf{A}_L] = \begin{bmatrix} [\mathbf{I}_{PQ} \otimes (\mathbf{H}_1 \mathbf{s})^T] \mathbf{K} \\ [\mathbf{I}_{PQ} \otimes (\mathbf{H}_2 \mathbf{s})^T] \mathbf{K} \\ \vdots \\ [\mathbf{I}_{PQ} \otimes (\mathbf{H}_L \mathbf{s})^T] \mathbf{K} \end{bmatrix}^T \\ &= \mathbf{K}^T \begin{bmatrix} (\mathbf{I}_{PQ} \otimes \mathbf{H}_1) \\ (\mathbf{I}_{PQ} \otimes \mathbf{H}_2) \\ \vdots \\ (\mathbf{I}_{PQ} \otimes \mathbf{H}_L) \end{bmatrix} (\mathbf{I}_{PQ} \otimes \mathbf{s}). \end{aligned} \quad (12)$$

Thus, the received signal in (8) can be rewritten as

$$\mathbf{r} = \sum_{l=1}^L \mathbf{A}_l \mathbf{x}_l + \mathbf{n} = \mathbf{A} \mathbf{x} + \mathbf{n} \quad (13)$$

where  $\mathbf{x} \triangleq [\mathbf{x}_1^T, \dots, \mathbf{x}_L^T]^T$  denotes a sparse vector, with the length being  $W \triangleq PQL$ .

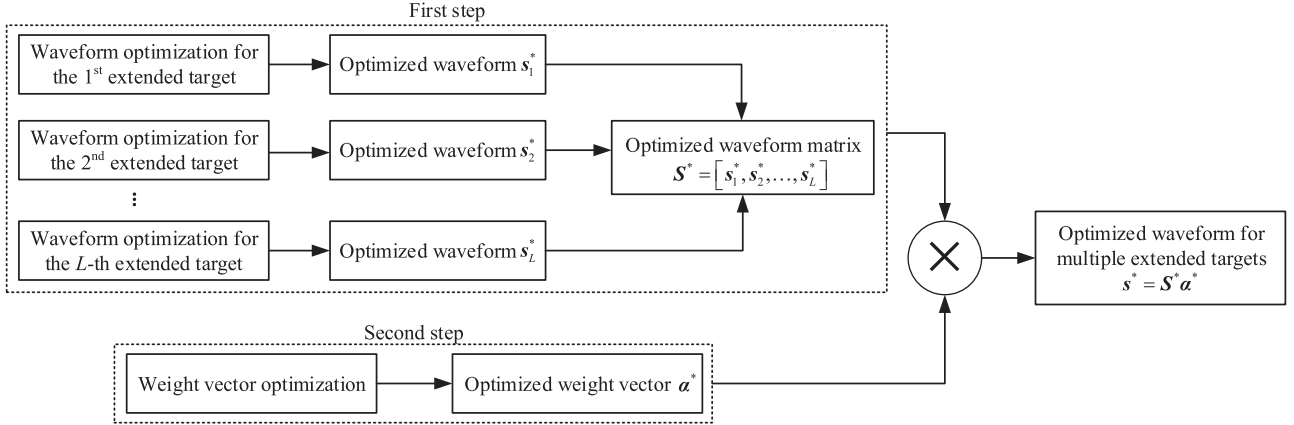


Fig. 3. Block diagram of the proposed two-step method to optimize the transmitted waveform.

When a sensing matrix  $\Phi \in \mathbb{R}^{M \times N_R}$  is adopted to measure the received signal  $\mathbf{r}$ , a compressed signal can be obtained as

$$\mathbf{y} = \Phi \mathbf{r} = \underbrace{\Phi \mathbf{A}}_{\Psi} \mathbf{x} + \underbrace{\Phi \mathbf{n}}_{\eta} \quad (14)$$

where  $\Psi \triangleq [\Psi_1, \Psi_2, \dots, \Psi_L]$ , and  $\Psi_l \triangleq \Phi \mathbf{A}_l$ . Generally, the entries of  $\Phi$  follow the Gaussian or random  $\pm 1$  distribution [30]. By exploiting the sparsity of  $\mathbf{x}$ , very few measurements are required to reconstruct the sparse vector  $\mathbf{x}$ , i.e.,  $M \ll N_R$ .

### III. WAVEFORM OPTIMIZATION

#### A. Mutual Coherence

To improve the performance of sparse reconstruction from the measured signal  $\mathbf{y}$ , a novel method is proposed here to optimize the transmitted waveform  $\mathbf{s}$ . When  $\Psi$  satisfies the RIP, recent advances in CS show that  $\mathbf{x}$  can be reconstructed from  $\mathbf{y}$  with a high probability. However, for a given matrix, there is no existing method with a polynomial complexity to check whether a matrix satisfies RIP. Thus, according to [31] and [32], the mutual coherence of  $\Psi$  is adopted as an alternative method to describe the reconstruction performance. The mutual coherence is defined as

$$\mu(\Psi) \triangleq \max_{i \neq j} \left\{ \frac{|\Psi^H(i) \Psi(j)|}{\|\Psi(i)\|_2 \|\Psi(j)\|_2} \right\} \quad (15)$$

where  $\Psi(i)$  denotes the  $i$ th  $j$ th column of  $\Psi$  ( $i \in \{1, 2, \dots, W\}$ ).

To minimize  $\mu(\Psi)$ , the transmitted waveform is optimized to minimize the off-diagonal entries of the following matrix [30]:

$$\mathbf{G} \triangleq \Psi^H \Psi = \mathbf{A}^H \Phi^H \Phi \mathbf{A} \approx \mathbf{A}^H \mathbf{A}. \quad (16)$$

The inequality in (16) is due to the fact that  $\Phi$  follows the standard Gaussian distribution implying that  $\Phi^H \Phi$  approximates an identity matrix. Then,  $\mu(\Psi)$  in (15) can be approximated as

$$\mu(\Psi) \approx \mu(\mathbf{G}) \triangleq \max_{i \neq j} \left\{ \frac{G_{ij}}{\sqrt{G_{ii} G_{jj}}} \right\} \quad (17)$$

where  $G_{ij}$  denotes the  $(i, j)$ th entry of  $\mathbf{G}$ .

#### B. Waveform Optimization

As shown in Fig. 3, a novel two-step method is proposed to optimize the transmitted waveform and to minimize the mutual coherence of the dictionary matrix. In the first step, the mutual coherence for each extended target is individually minimized, and the optimized waveforms are obtained. In the second step, a weight vector is obtained by another iteration method. Then, for multiple extended targets, the finally transmitted waveform is obtained by combing the optimized waveforms in the first step with the optimized weight vector. The details are given as follows.

1) *First Step (Individual Optimization)*: For the  $l$ th extended target, the following result can be obtained from (9) and (16):

$$\mathbf{G}_l \triangleq \Psi_l^H \Psi_l = (\mathbf{I}_{PQ} \otimes \mathbf{H}_l \mathbf{s})^H (\mathbf{K} \mathbf{K}^H)^T [\mathbf{I}_{PQ} \otimes (\mathbf{H}_l \mathbf{s})].$$

Therefore, the waveform design for the  $l$ th target can be represented by an optimization problem under the transmit power constraint, i.e.,

$$\begin{aligned} \min_{\mathbf{s}} \quad & \mu(\mathbf{G}_l) \\ \text{s.t.} \quad & \|\mathbf{s}\|_2^2 \leq E_s \end{aligned} \quad (18)$$

where  $E_s$  denotes the maximum transmitted power. We define a diagonal matrix  $\tilde{\mathbf{G}}_l$  with the diagonal entries being the same with  $\mathbf{G}_l$ . If the columns of  $\Psi$  are orthogonal to each other, all the off-diagonal entries in  $\mathbf{G}_l$  will be zero, leading  $\mathbf{G}_l$  to be  $\tilde{\mathbf{G}}_l$ . Therefore, to minimize  $\mu(\Psi)$ , the correlation between the columns of  $\mathbf{G}_l$  must be as less as possible. Then, the following equivalent optimization problem can be obtained

$$\begin{aligned} \min_{\mathbf{s}} \quad & \|\mathbf{G}_l - \tilde{\mathbf{G}}_l\|_{\max} \\ \text{s.t.} \quad & \|\mathbf{s}\|_2^2 \leq E_s \end{aligned} \quad (19)$$

where  $\|\mathbf{A}\|_{\max} \triangleq \max_{i,j} \{|A_{ij}|\}$  denotes the maximum absolute value among all the entries of  $\mathbf{A}$ .

Since the optimization problem (19) is nonconvex and cannot be solved efficiently, Equation (19) can be converted into [33]

$$\begin{aligned} \min_{\mathbf{s}} \quad & \|\mathbf{G}_l - \tilde{\mathbf{G}}_l\|_F \\ \text{s.t.} \quad & \|\mathbf{s}\|_2^2 \leq E_s \end{aligned} \quad (20)$$

where the Frobenius norm is defined as  $\|\mathbf{A}\|_F \triangleq \sqrt{\sum_i \sum_j |A_{ij}|^2}$ . To solve (20), an iterative method is proposed as follows:

- 1) Since all the diagonal entries of both  $\mathbf{G}_l$  and  $\tilde{\mathbf{G}}_l$  are nonnegative,  $\tilde{\mathbf{G}}_l$  can be decomposed as

$$\tilde{\mathbf{G}}_l = \tilde{\mathbf{G}}_l'^H \mathbf{U}_l^H \mathbf{U}_l \tilde{\mathbf{G}}_l'$$

where  $\tilde{\mathbf{G}}_l' \triangleq \text{diag}\{\sqrt{G_{11}}, \sqrt{G_{22}}, \dots, \sqrt{G_{NN}}\}$ , and  $\mathbf{U}_l$  is a unitary matrix with  $\mathbf{U}_l^H \mathbf{U}_l = \mathbf{I}$ . Note that  $\mathbf{G}_l = \Psi_l^H \tilde{\mathbf{G}}_l'$  according to (18), and (20) can be converted to

$$\begin{aligned} \min_{\mathbf{U}_l, \mathbf{s}} f(\mathbf{U}_l, \mathbf{s}) \\ \text{s.t. } \|\mathbf{s}\|_2^2 \leq E_s \end{aligned}$$

where  $f(\mathbf{U}_l, \mathbf{s}) \triangleq \|\Psi_l - \mathbf{U}_l \tilde{\mathbf{G}}_l'\|_F$ .

- 2) Substituting (18) into  $f(\mathbf{U}_l, \mathbf{s})$ , we have

$$f(\mathbf{U}_l, \mathbf{s}) = \left\| \mathbf{K}^T [\mathbf{I}_{PQ} \otimes (\mathbf{H}_l \mathbf{s})] - \mathbf{U}_l \tilde{\mathbf{G}}_l' \right\|_F.$$

- 3) For a given waveform  $\mathbf{s}$ , the unitary matrix  $\mathbf{U}_l$  minimizing  $f(\mathbf{U}_l, \mathbf{s})$  is

$$\mathbf{U}_l^* = \mathbf{U}_{l,1} \mathbf{U}_{l,2}^H$$

where  $\mathbf{U}_{l,1}$  and  $\mathbf{U}_{l,2}^H$  are unitary matrices satisfying [34]

$$\mathbf{K}^T [\mathbf{I}_{PQ} \otimes (\mathbf{H}_l \mathbf{s})] \tilde{\mathbf{G}}_l'^{-1} = \mathbf{U}_{l,1} \Sigma_l \mathbf{U}_{l,2}^H.$$

- 4) After obtaining  $\mathbf{U}_l^*$ , we have

$$\begin{aligned} f(\mathbf{U}_l^*, \mathbf{s}_l) &= \left\| \mathbf{K}^T [\mathbf{I}_{PQ} \otimes (\mathbf{H}_l \mathbf{s})] - \mathbf{U}_l^* \tilde{\mathbf{G}}_l' \right\|_F \\ &= \left\| \mathbf{K}'(\mathbf{H}_l \mathbf{s}) - \text{vec} \left\{ \mathbf{U}_l^* \tilde{\mathbf{G}}_l' \right\} \right\|_2 \end{aligned}$$

where  $\text{vec}(\cdot)$  denotes a column vector by stacking the columns of a matrix together, and

$$\mathbf{K}' \triangleq \begin{bmatrix} M(0 \cdot \Delta f_D) \mathbf{D}(0 \cdot \Delta \tau) \\ \vdots \\ M((Q-1) \cdot \Delta f_D) \mathbf{D}(0 \cdot \Delta \tau) \\ \vdots \\ M((Q-1) \cdot \Delta f_D) \mathbf{D}(1 \cdot \Delta \tau) \\ \vdots \\ M((Q-1) \cdot \Delta f_D) \mathbf{D}((P-1) \cdot \Delta \tau) \end{bmatrix}.$$

Minimize  $f(\mathbf{U}_l^*, \mathbf{s}_l)$ , and the optimized waveform  $\mathbf{s}_l^*$  for the  $l$ th extended target can be obtained as

$$\mathbf{s}_l^* = (\mathbf{K}' \mathbf{H}_l)^+ \text{vec} \left\{ \mathbf{U}_l^* \tilde{\mathbf{G}}_l' \right\}.$$

where  $(\cdot)^+$  denotes the Moore–Penrose pseudoinverse of a matrix.

- 5) If the maximum iteration number is not reached and the mutual coherence decreases, go to Step 3 to obtain a

new unitary matrix and iteratively perform Steps 3 and 4; otherwise, output  $\mathbf{s}_l^*$ .

- 2) *Second Step (Weight Vector Optimization)*: After  $\mathbf{s}_l^*$  ( $l = 1, 2, \dots, L$ ) is obtained for all the extended targets at the first step, a weight vector  $\boldsymbol{\alpha} = [\alpha_1, \alpha_2, \dots, \alpha_L]^T$  can be adopted to design the optimized waveform  $\mathbf{s}^*$

$$\mathbf{s}^* = \sqrt{E_s} \frac{\mathbf{S}^* \boldsymbol{\alpha}}{\|\mathbf{S}^* \boldsymbol{\alpha}\|_2} \quad (21)$$

where waveform matrix  $\mathbf{S}^* \triangleq [\mathbf{s}_1^*, \mathbf{s}_2^*, \dots, \mathbf{s}_L^*]$ . To optimize  $\boldsymbol{\alpha}$ , an iteration algorithm is proposed in Algorithm 1, and the optimized weight vector  $\boldsymbol{\alpha}^*$  is obtained as the output of Algorithm 1. Then, the optimized waveform is  $\mathbf{s}^* = \mathbf{S}^* \boldsymbol{\alpha}^*$ .

---

#### Algorithm 1 Weight Vector Optimization for Multiple Extended Targets

---

- 1: *Input*: optimized waveform matrix  $\mathbf{S}^*$ , transmit power  $E_s$ , step  $\delta$ , maximum iteration number  $K$ , number of targets  $L$ .
  - 2: *Initialization*:  $\boldsymbol{\alpha}_0 = \mathbf{1}_L$ .
  - 3: **for**  $k = 0, \dots, K - 1$  **do**
  - 4:  $\mathbf{s}_k = (\sqrt{E_s} \mathbf{S}^* \boldsymbol{\alpha}_k / \|\mathbf{S}^* \boldsymbol{\alpha}_k\|_2)$ .
  - 5: With  $\mathbf{s}_k$ , obtain dictionary matrix  $\mathbf{A}_{k,l}$  ( $1 \leq l \leq L$ ) from (9).
  - 6: Generate Gaussian random matrix  $\Phi$ .
  - 7:  $\Psi_{k,l} = \Phi \mathbf{A}_{k,l}$  ( $1 \leq l \leq L$ ), and  $\Psi_k \triangleq [\Psi_{k,1}, \Psi_{k,2}, \dots, \Psi_{k,L}]$ .
  - 8:  $\mathbf{G}_k = \Psi_k^H \Psi_k$ .
  - 9: Obtain  $\mu(\mathbf{G}_k)$  from (17).
  - 10:  $\boldsymbol{\alpha}_a = \boldsymbol{\alpha}_k$ ,  $\boldsymbol{\alpha}_s = \boldsymbol{\alpha}_k$ ,  $\boldsymbol{\alpha}_{k+1} = \boldsymbol{\alpha}_k$ , and  $\mu(\mathbf{G}_{k+1}) = \mu(\mathbf{G}_k)$ .
  - 11: **for**  $l = 1, \dots, L$  **do**
  - 12:  $\tilde{\boldsymbol{\alpha}}_a = \boldsymbol{\alpha}_a$ , and  $[\tilde{\boldsymbol{\alpha}}_a]_l = [\tilde{\boldsymbol{\alpha}}_a]_l + \delta$ .
  - 13:  $\tilde{\boldsymbol{\alpha}}_s = \boldsymbol{\alpha}_s$ , and  $[\tilde{\boldsymbol{\alpha}}_s]_l = [\tilde{\boldsymbol{\alpha}}_s]_l - \delta$ .
  - 14:  $\mathbf{s}_a = (\sqrt{E_s} \mathbf{S}^* \tilde{\boldsymbol{\alpha}}_a / \|\mathbf{S}^* \tilde{\boldsymbol{\alpha}}_a\|_2)$ .
  - 15:  $\mathbf{s}_s = (\sqrt{E_s} \mathbf{S}^* \tilde{\boldsymbol{\alpha}}_s / \|\mathbf{S}^* \tilde{\boldsymbol{\alpha}}_s\|_2)$ .
  - 16: With  $\mathbf{s}_a$ , obtain dictionary matrix  $\mathbf{A}_{a,l}$  ( $1 \leq l \leq L$ ) from (9).
  - 17: With  $\mathbf{s}_s$ , obtain dictionary matrix  $\mathbf{A}_{s,l}$  ( $1 \leq l \leq L$ ) from (9).
  - 18:  $\Psi_{a,l} = \Phi \mathbf{A}_{a,l}$  ( $1 \leq l \leq L$ ), and  $\Psi_a \triangleq [\Psi_{a,1}, \Psi_{a,2}, \dots, \Psi_{a,L}]$ .
  - 19:  $\Psi_{s,l} = \Phi \mathbf{A}_{s,l}$  ( $1 \leq l \leq L$ ), and  $\Psi_s \triangleq [\Psi_{s,1}, \Psi_{s,2}, \dots, \Psi_{s,L}]$ .
  - 20:  $\mathbf{G}_a = \Psi_a^H \Psi_a$  and  $\mathbf{G}_s = \Psi_s^H \Psi_s$ .
  - 21: Obtain  $\mu(\mathbf{G}_a)$  and  $\mu(\mathbf{G}_s)$  from (17).
  - 22:  $\mathbf{c}_1 = \boldsymbol{\alpha}_{k+1}$ ,  $\mathbf{c}_2 = \boldsymbol{\alpha}_a$ , and  $\mathbf{c}_3 = \boldsymbol{\alpha}_s$ .
  - 23:  $\mu_1 = \mu(\mathbf{G}_{k+1})$ ,  $\mu_2 = \mu(\mathbf{G}_a)$ , and  $\mu_3 = \mu(\mathbf{G}_s)$ .
  - 24:  $i^* = \arg \min_i \{\mu_i\}$ .
  - 25:  $\mu(\mathbf{G}_{k+1}) \leftarrow \mu_{i^*}$ ,  $\boldsymbol{\alpha}_{k+1} \leftarrow \mathbf{c}_{i^*}$ ,  $\boldsymbol{\alpha}_a \leftarrow \mathbf{c}_{i^*}$ , and  $\boldsymbol{\alpha}_s \leftarrow \mathbf{c}_{i^*}$ .
  - 26: **end for**
  - 27: **if**  $\boldsymbol{\alpha}_k = \boldsymbol{\alpha}_{k+1}$  **then**
  - 28: Break.
  - 29: **end if**
  - 30: **end for**
  - 31: *Output*: optimized weight vector  $\boldsymbol{\alpha}^* = \boldsymbol{\alpha}_k$ .
-

TABLE I  
SIMULATION PARAMETERS

Parameter	Value
Range resolution	50 m
Velocity resolution	10 m/s
The number of range bins	10
The number of velocity bins	10
The compression ratio	4 : 5
The target number	3
The transmit power $E_s$	1

In Algorithm 1, the vector with all entries being 1 is used as an initial waveform weight vector  $\alpha_0$ . Then, a step  $\delta$  is used to fix the weight vector iteratively. At the  $k$ th iterative step, two new weight vectors  $\alpha_a$  and  $\alpha_s$  are calculated by adding and subtracting one entry of  $\alpha_k$  with the step  $\delta$ . Therefore, three waveforms with weight vectors  $\alpha_k$ ,  $\alpha_a$ , and  $\alpha_s$  can be obtained, i.e.,  $s_k$ ,  $s_a$ , and  $s_s$ . Then, the dictionary matrices  $\Psi_k$ ,  $\Psi_a$ , and  $\Psi_s$  for all extended targets with the corresponding waveforms  $s_k$ ,  $s_a$ , and  $s_s$  can be obtained. By calculating the mutual coherence of all dictionary matrices, the waveform and the corresponding weight vector which achieve the minimum mutual coherence can be obtained, and this weight vector is used for the next iteration and denoted  $\alpha_{k+1}$ . If  $\alpha_{k+1} = \alpha_k$ , stop the iteration and the optimized weight vector  $\alpha^* = \alpha_k$  is achieved, and the optimized waveform can be calculated by (21).

In Algorithm 1, the step  $\delta$  is used to control the convergence of calculating the weight vector  $\alpha$ . Since the minimum mutual coherence is chosen at each iteration step, the mutual coherence is monotone decreasing. Therefore, increasing  $\delta$  appropriately can improve the convergence rate. The simulation results for different  $\delta$  are given in Fig. 6 in Section IV. Therefore, for both the convergence and accuracy consideration, an appropriate  $\delta$  need to be chosen, and we choose  $\delta = 10^{-2}$  under our simulation conditions.

#### IV. SIMULATION RESULTS

##### A. Waveform Optimization to Minimize the Mutual Coherence

First, we evaluate the proposed method to optimized the transmitted waveform, and the simulation parameters are given in Table I. For realistic consideration, the simulation parameters in this paper are chosen according to [26], [28], and [35]–[37], where the typical CS-based radar systems are described. In the initial simulations, the SNR of the received signal is set to be 20 dB, which can be changed for the different system realizations. Additionally, if there are no additional statements, the simulation parameters are the same with Table I.

In the proposed two-step method, the waveform is first individually optimized for each extended target. As shown in Fig. 4, the waveforms are optimized for three extended targets, and all the mutual coherences are decreasing with the optimization iterations. Additionally, the optimization processes with different initial waveforms are also shown, where choosing different initial waveforms has a limited effect on the final converged mutual coherence. Therefore, the proposed first step of waveform optimization is not sensitive with the initial waveforms.

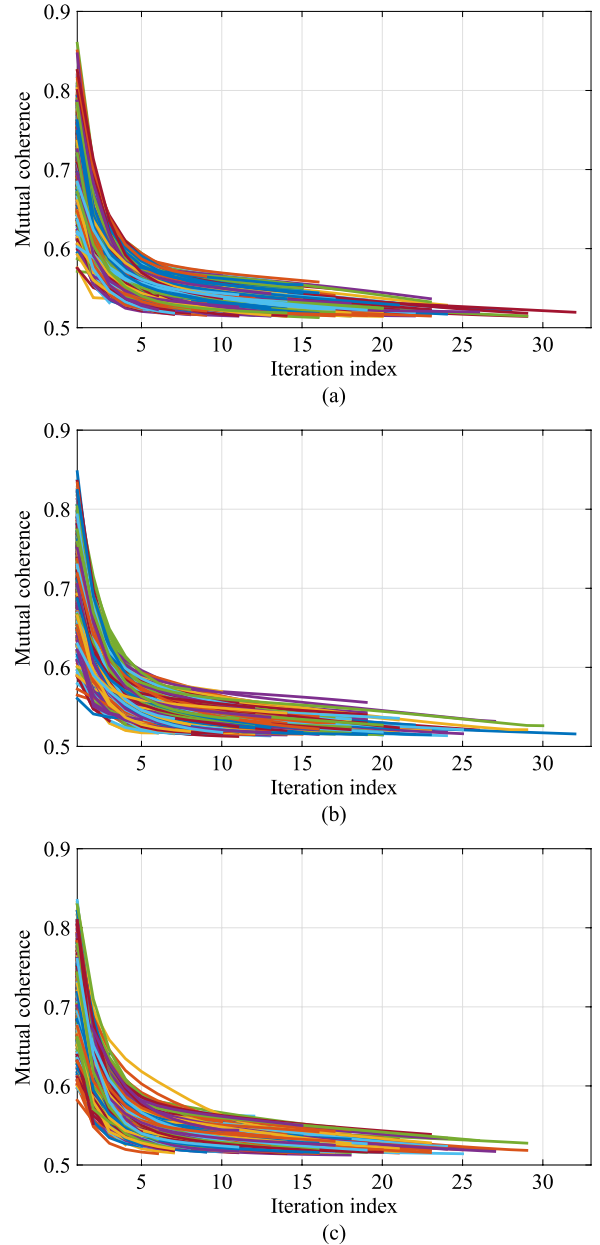


Fig. 4. Waveform optimization for different extended targets at the first step of proposed method. (a) Waveform optimization for target 1 with different initial waveforms. (b) Waveform optimization for target 2 with different initial waveforms. (c) Waveform optimization for target 3 with different initial waveforms.

Then, in the practical radar system, multiple random waveforms can be adopted as the initial waveforms at the first step of the iterative method. Then, the waveform with the minimal mutual coherence is chosen as the optimal one for each extended targets.

After obtaining the optimized waveform for each extended target, the dictionary matrices for different targets and waveforms can be obtained from (18), and the corresponding mutual coherences can be also obtained. As shown in Fig. 5, the mutual coherences of three optimized waveforms for the corresponding three extended targets are shown, and the optimized waveforms for the corresponding targets cannot guarantee the minimal mutual coherence for other targets. Therefore, the following steps to combine these optimization waveforms are necessary.

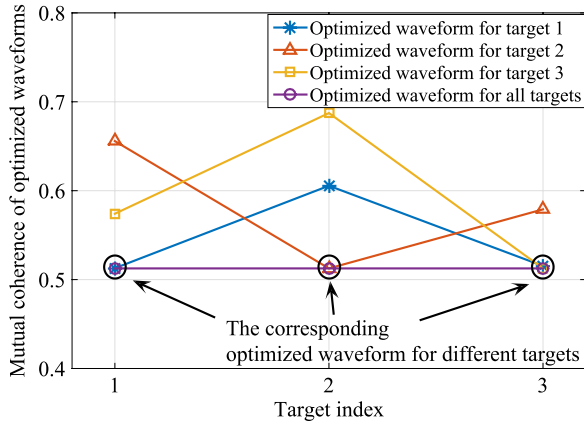


Fig. 5. Mutual coherence of different optimized waveforms.

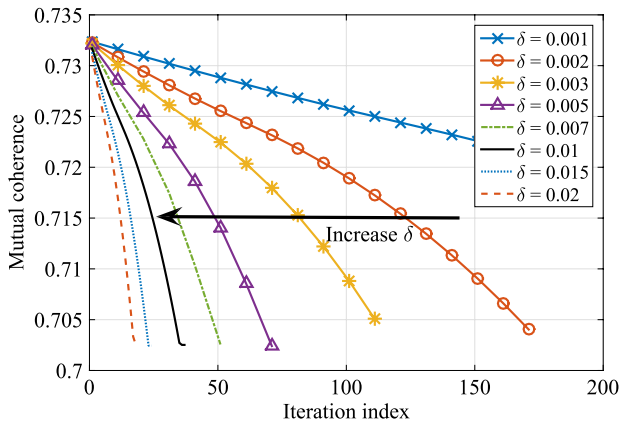


Fig. 6. Obtaining the weight vector with different steps  $\delta$ .

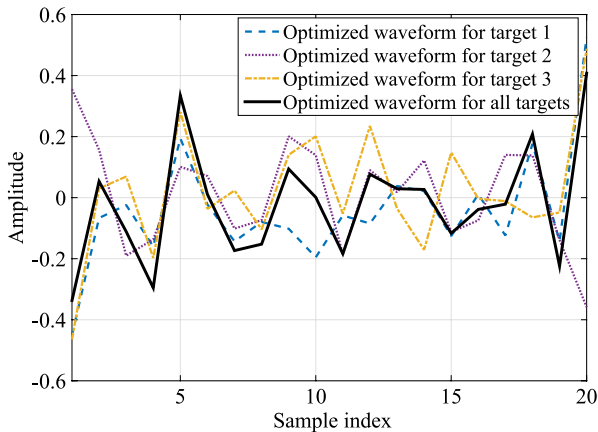


Fig. 7. Optimized waveform for multiple extended targets.

In the second step of the two-step method, a weight vector is obtained to combine the first individually optimized waveforms. As shown in Fig. 6, the iterative processes to calculate the weight vector are depended on the step  $\delta$  in Algorithm 1. For both convergence and accuracy considerations,  $\delta = 10^{-2}$  is used in this paper. Finally,  $\alpha^* = [0.8359, 0.6189, 0.3901]^T$  is obtained as the weight vector, and the optimized radar waveforms are shown in Fig. 7, where optimized waveform

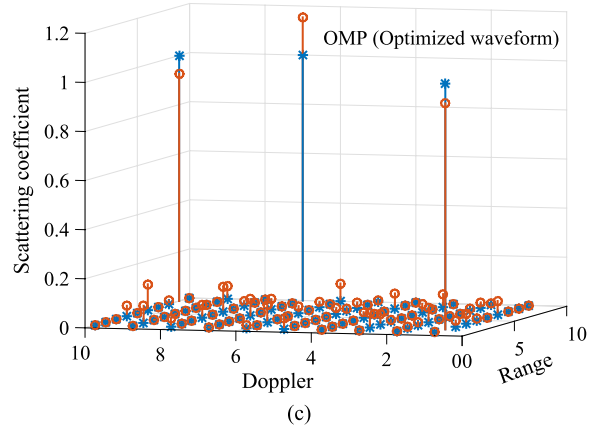
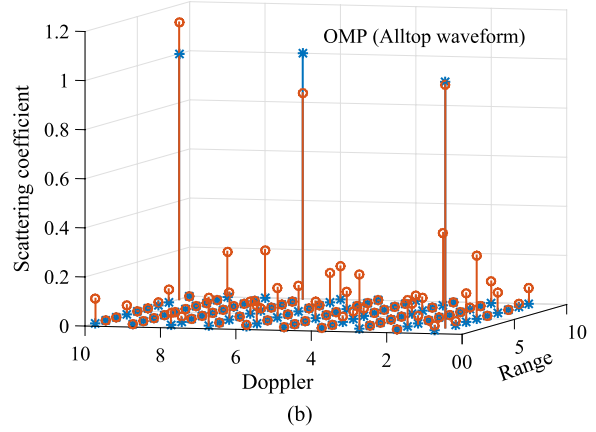
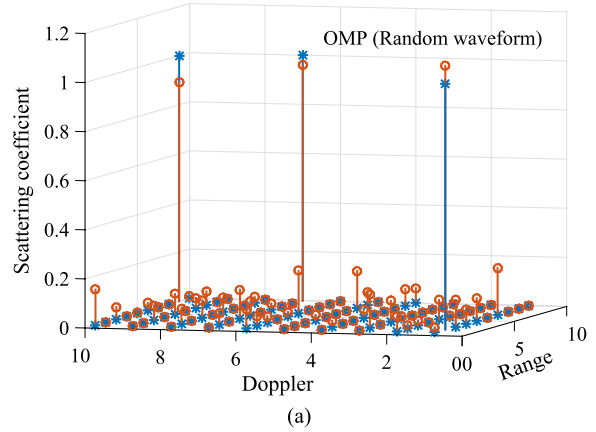


Fig. 8. Sparse reconstruction in the delay–Doppler plane using OMP method. (a) Random waveform. (b) Alltop waveform. (c) Optimized waveform.

for all extended targets are different from the ones for individual targets. Additionally, the mutual coherence of optimized waveform is shown in Fig. 5, where the finally optimized waveform achieves the best mutual coherence performance for all extended targets at the same time.

The classical CS algorithms including orthogonal matching pursuit (OMP) and basis pursuit (BP) [31], [39] are adopted to reconstruct the sparse vector. The comparisons between the original and reconstructed scattering coefficients in the delay–Doppler plane using OMP and BP are shown in Figs. 8 and 9, respectively. As shown in Figs. 8(a) and 9(a), the random waveforms are adopted as the transmitted waveform. In

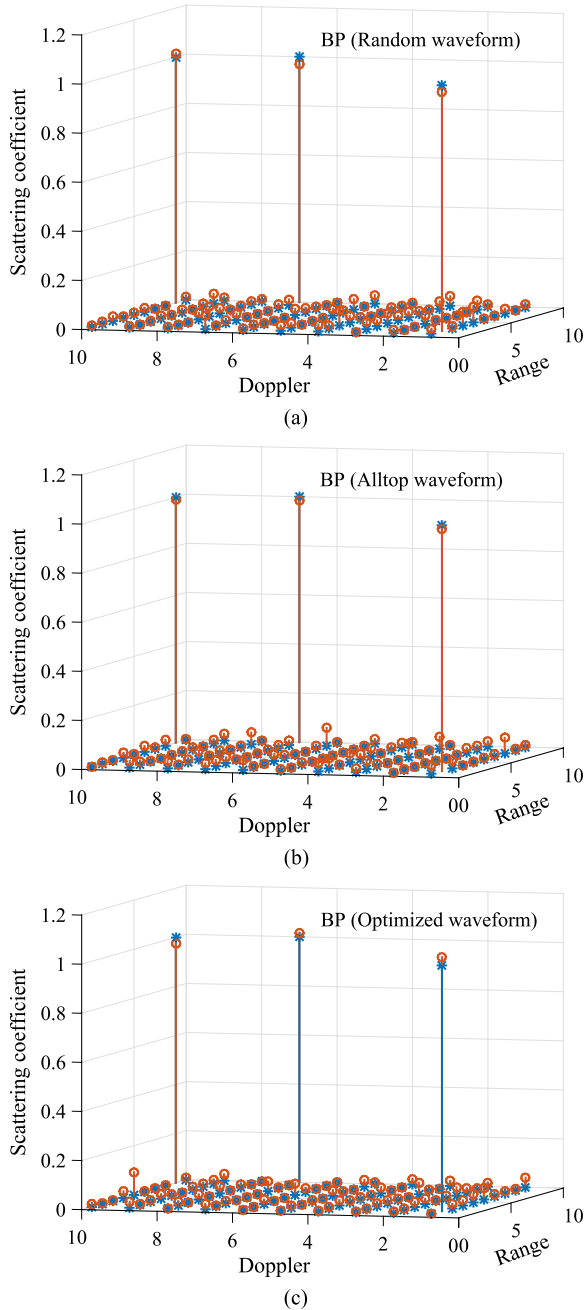


Fig. 9. Sparse reconstruction in the delay–Doppler plane using BP method. (a) Random waveform. (b) Alltop waveform. (c) Optimized waveform.

Figs. 8(b) and 9(b), the Alltop sequence is used as the transmitted waveform. The Alltop sequence is defined in [39] and [40]

$$s_A(n) = \frac{1}{\sqrt{N}} e^{j \frac{2\pi}{N} n^3}, \quad n = 1, 2, \dots, N \quad (22)$$

where  $N$  denotes the sample number of the transmitted waveform. The Alltop sequence has the ideal autocorrelation characteristics in the traditional radar system. In Figs. 8(c) and 9(c), we optimize the transmitted waveform using the proposed method. It is observed that the optimized waveform performs better than both the random and Alltop waveforms when either the OMP or BP reconstruction method is adopted. However, as

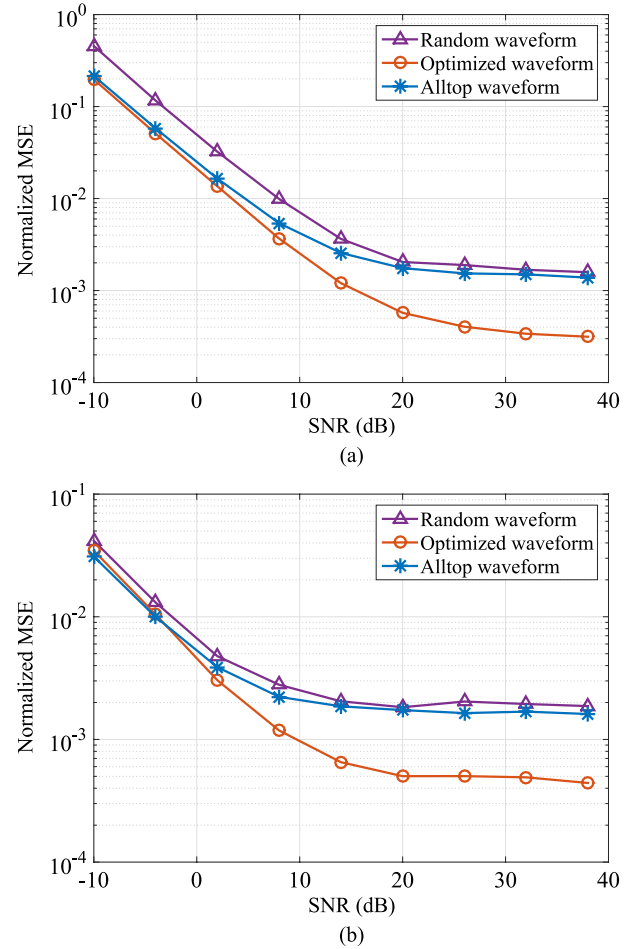


Fig. 10. Sparse reconstruction performance with different SNRs. (a) Sparse reconstruction using OMP. (b) Sparse reconstruction using BP.

in this simulation the SNR of the received signal is up to 20 dB for the clear illustration, the advantages are not very clear. Therefore, In the following, these three transmitted waveforms will be compared in details in terms of normalized mses under different conditions of SNR, target numbers, and measurement numbers.

### B. Estimation of Extended Targets With Different SNR

We compare the estimation performance of extended targets at different SNR for random, Alltop, and optimized waveforms. As shown in Fig. 10, we provide the normalized mse of the sparse reconstruction using OMP and BP. It is shown in Fig. 10(a) using OMP that, the transmitted waveform using the proposed method always performs better than both random and Alltop waveforms, particularly at SNR of  $> 15$  dB. In Fig. 10(b) using BP, it is seen that the proposed radar waveform optimization method significantly outperforms random and Alltop waveforms at high SNR region (SNR  $> 10$  dB). In both Fig. 10(a) and (b), the floor effect due to the noise is less obvious for the proposed optimized waveform than random and Alltop waveforms, indicating that the proposed method is more effective at high SNR region.

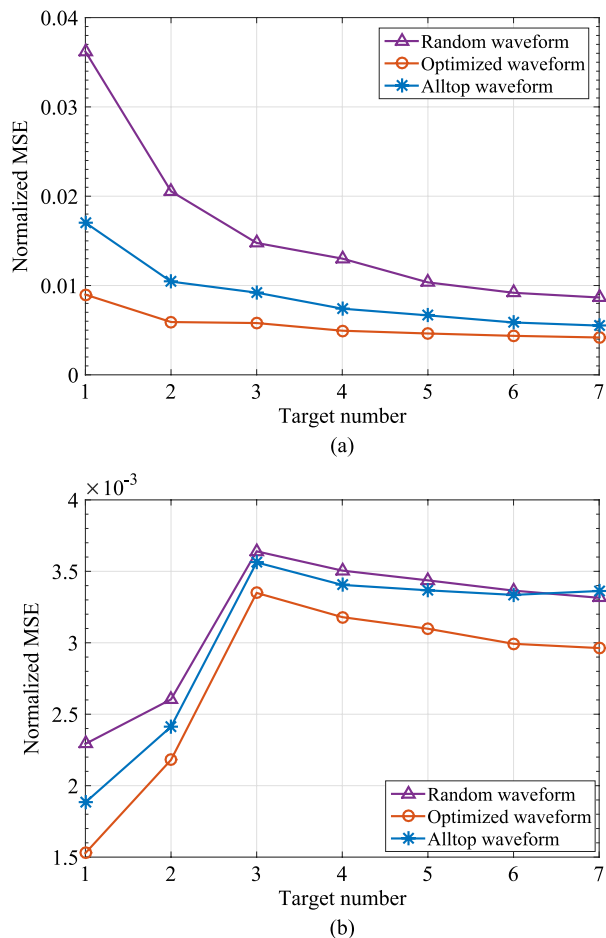


Fig. 11. Sparse reconstruction performance with different target numbers. (a) Sparse reconstruction using OMP. (b) Sparse reconstruction using BP.

C. Estimation of Extended Targets With Different Target Numbers

We compare the estimation performance of extended targets with different targets numbers for random, Alltop and optimized waveforms, where the SNR of the received signal is 5 dB. As shown in Fig. 11, we provide the normalized mse of the sparse reconstruction using OMP and BP. It is shown in Fig. 11(a) using OMP that, the transmitted waveform using the proposed method performs much better than random and Alltop waveforms when the target number is from 1 to 7. Additionally, in Fig. 11(b) using BP, we observe that the optimized waveform is the best among the three different waveforms for the target number from 1 to 7. Therefore, by using the waveform optimization method, which reducing the mutual coherence of dictionary matrix, the sparse reconstruction can be improved with different target numbers when the general CS reconstruction algorithms are used.

D. Estimation of Extended Targets With Different Measurement Numbers

The estimation performances of extended targets with different measurement numbers are compared for random, Alltop and optimized waveforms. As shown in Fig. 12, we provide the

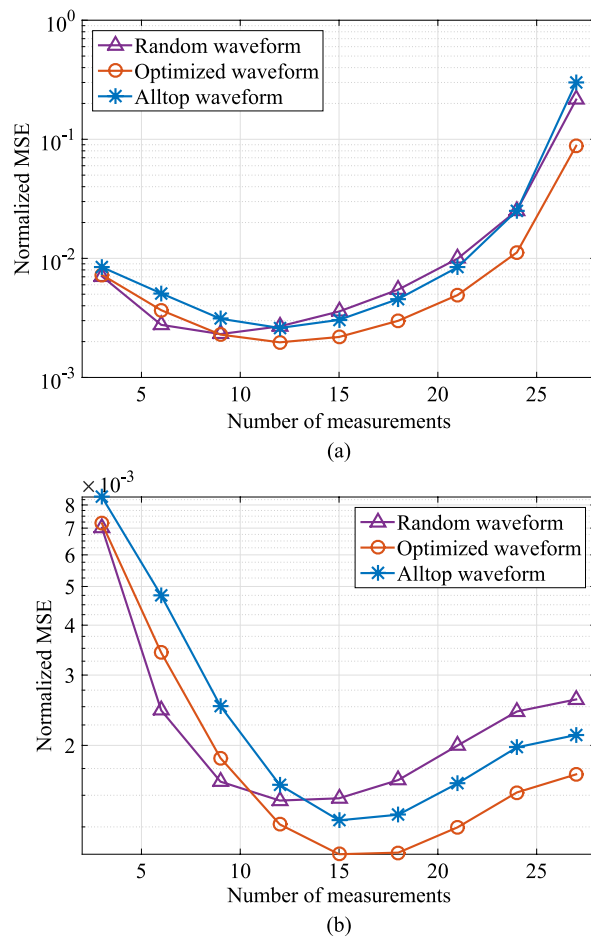


Fig. 12. Sparse reconstruction performance with different measurement numbers. (a) Sparse reconstruction using OMP. (b) Sparse reconstruction using BP.

normalized mse of the sparse reconstruction using OMP and BP, where the SNR of the received signal is 8 dB. We observe from both Fig. 12(a) and (b) that, the normalized MSE is the smallest when the number of measurements is  $M = 15$ . Either  $M$  too small or too large increases the normalized MSE. In fact, if  $M$  is too small, the measurements are not enough to obtain an accurate estimate for the sparse reconstruction. If  $M$  is too large, the mutual coherence of measurement matrix will also increase, leading to the performance reduction. Specially, it is shown in Fig. 12(a) using OMP that, if  $M > 10$ , the transmitted waveform using the proposed method outperforms random waveform and Alltop waveform. It is shown in Fig. 12(b) using BP that, if  $M \geq 12$ , the transmitted waveform using the proposed method outperforms random and Alltop waveforms.

V. DISCUSSIONS

To illustrate the effects of target number and measurement number, the sparse reconstruction performance with different target numbers or measurement numbers is shown in Fig. 13, where the OMP algorithm is used in Fig. 13(a) and BP algorithm is used in Fig. 13(b). When OMP algorithm is used, the best measurement number increases with the target number. However, since the TIRs and optimized waveforms are different among extended targets, neither increasing the measurement

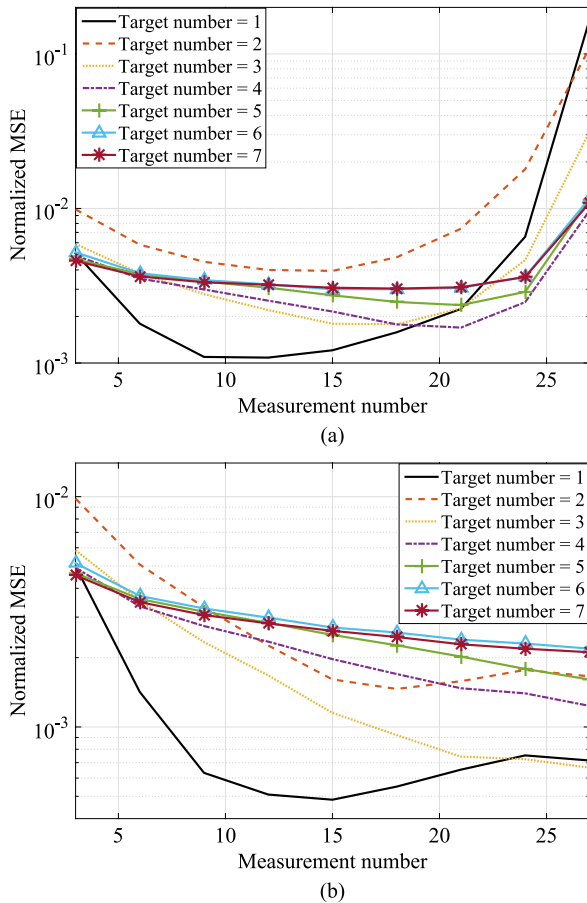


Fig. 13. Sparse reconstruction performance for the consideration of both target number and measurement number. (a) Sparse reconstruction using OMP. (b) Sparse reconstruction using BP.

number nor decreasing the target number can guarantee the increasing of reconstruction performance. Therefore, for different target numbers, the measurement number must be chosen appropriately. When the BP algorithm is used, as shown in Fig. 13(b), either increasing the measurement number or decreasing the target number usually can improve the sparse reconstruction performance. In our simulation results, for both OMP and BP algorithms, when the number of extended targets is chosen from 1 to 7, the best measurement number is around 20. Note that more considerations about the measurement number must be taken in the different scenarios.

## VI. CONCLUSION

In this paper, a radar system model based on CS has been established for multiple extended targets in the delay-Doppler plane. Then, both OMP and BP algorithms have been adopted to estimate the target ranges and velocities. Additionally, to minimize the mutual coherence of the dictionary matrix and improve the estimation performance, an iterative two-step method has also been proposed. Simulation results show the convergence of the proposed iterative algorithm and the performance improvement achieved by optimizing the transmitted waveform. Future work will concentrate on the waveform optimization for multiple extended targets in the CS radar with clutters.

## REFERENCES

- [1] J. Paredes, G. Arce, and Z. Wang, "Ultra-wideband compressed sensing: Channel estimation," *IEEE J. Sel. Topics Signal Process.*, vol. 1, no. 3, pp. 383–395, Oct. 2007.
- [2] A. Gurbuz, J. McClellan, and W. Scott, "A compressive sensing data acquisition and imaging method for stepped frequency GPRs," *IEEE Trans. Signal Process.*, vol. 57, no. 7, pp. 2640–2650, Jul. 2009.
- [3] E. Candes and M. Wakin, "An introduction to compressive sampling," *IEEE Signal Process. Mag.*, vol. 25, no. 2, pp. 21–30, Mar. 2008.
- [4] R. Baraniuk, "Compressive sensing," *IEEE Signal Process. Mag.*, vol. 24, no. 4, pp. 118–121, Jul. 2007.
- [5] J. Haupt and R. Nowak, "Signal reconstruction from noisy random projections," *IEEE Trans. Inf. Theory*, vol. 52, no. 9, pp. 4036–4048, Sep. 2006.
- [6] Z. Zhang, T. K. Chan, and K. H. Li, "A semidefinite relaxation approach for beamforming in cooperative clustered multicell systems with novel limited feedback scheme," *IEEE Trans. Veh. Technol.*, vol. 63, no. 4, pp. 1740–1748, May 2014.
- [7] Y. Yao, A. P. Petropulu, and H. V. Poor, "MIMO radar using compressive sampling," *IEEE J. Sel. Areas Signal Process.*, vol. 4, no. 1, pp. 146–163, Feb. 2010.
- [8] I. Kyriakides, "Adaptive compressive sensing and processing of delay-Doppler radar waveforms," *IEEE Trans. Signal Process.*, vol. 60, no. 2, pp. 730–739, Feb. 2012.
- [9] Y. Yu, A. P. Petropulu, and H. V. Poor, "CSSF MIMO radar: Compressive-sensing and step-frequency based MIMO radar," *IEEE Trans. Aerosp. Electron. Syst.*, vol. 48, no. 2, pp. 1490–1504, Apr. 2012.
- [10] S. Haykin, "Cognitive radar: A way of the future," *IEEE Signal Process. Mag.*, vol. 23, no. 1, pp. 30–40, Jan. 2006.
- [11] A. Leshem, O. Napshtek, and A. Nehorai, "Information theoretic adaptive radar waveform design for multiple extended targets," *IEEE J. Sel. Topics Signal Process.*, vol. 1, no. 1, pp. 42–55, Jun. 2007.
- [12] Y. Yang and R. Blum, "MIMO radar waveform design based on mutual information and minimum mean-square error estimation," *IEEE Trans. Aerosp. Electron. Syst.*, vol. 43, no. 1, pp. 330–343, Jan. 2007.
- [13] Y. Nijsure *et al.*, "Novel system architecture and waveform design for cognitive radar radio networks," *IEEE Trans. Veh. Technol.*, vol. 61, no. 8, pp. 3630–3642, Oct. 2012.
- [14] X. Cheng, M. Wang, and Y. L. Guan, "Ultra-wideband channel estimation: A Bayesian compressive sensing strategy based on statistical sparsity," *IEEE Trans. Veh. Technol.*, vol. 64, no. 5, pp. 1819–1832, May 2015.
- [15] W. Zhu and J. Tang, "Robust design of transmit waveform and receive filter for colocated MIMO radar," *IEEE Signal Process. Lett.*, vol. 22, no. 11, pp. 2112–2116, Jul. 2015.
- [16] M. Naghsh *et al.*, "A Doppler robust design of transmit sequence and receive filter in the presence of signal-dependent interference," *IEEE Trans. Signal Process.*, vol. 62, no. 4, pp. 772–785, Feb. 2014.
- [17] W. Huleihel, J. Tabrikian, and R. Shavit, "Optimal adaptive waveform design for cognitive MIMO radar," *IEEE Trans. Signal Process.*, vol. 61, no. 20, pp. 5075–5089, Oct. 2013.
- [18] P. Chavali and A. Nehorai, "Scheduling and power allocation in a cognitive radar network for multiple-target tracking," *IEEE Trans. Signal Process.*, vol. 60, no. 2, pp. 715–729, Dec. 2012.
- [19] Y. Junkun, J. Bo, L. Hongwei, C. Bo, and B. Zheng, "Prior knowledge-based simultaneous multibeam power allocation algorithm for cognitive multiple targets tracking in clutter," *IEEE Trans. Signal Process.*, vol. 63, no. 2, pp. 512–527, Dec. 2015.
- [20] S. Wang, Q. He, and Z. He, "LFM-based waveform design for cognitive MIMO radar with constrained bandwidth," *EURASIP J. Adv. Signal Process.*, vol. 2014, no. 1, pp. 1–9, Jun. 2014.
- [21] L. Xia *et al.*, "Demonstration of cognitive radar for target localization under interference," *IEEE Trans. Aerosp. Electron. Syst.*, vol. 50, no. 4, pp. 2440–2455, Oct. 2014.
- [22] J. Liu, H. Li, and B. Himed, "Joint optimization of transmit and receive beamforming in active arrays," *IEEE Signal Process. Lett.*, vol. 21, no. 1, pp. 39–42, Nov. 2014.
- [23] J. Ender, "A brief review of compressive sensing applied to radar," in *Proc. 14th Int. Radar Symp.*, Jun. 2013, pp. 3–16.
- [24] T. Zhao, Y. Peng, and A. Nehorai, "Joint sparse recovery method for compressed sensing with structured dictionary mismatches," *IEEE Trans. Signal Process.*, vol. 62, no. 19, pp. 4997–5008, Jul. 2014.
- [25] Y. Yu, S. Sun, R. N. Madan, and A. Petropulu, "Power allocation and waveform design for the compressive sensing based MIMO radar," *IEEE Trans. Aerosp. Electron. Syst.*, vol. 50, no. 2, pp. 898–909, Apr. 2014.
- [26] S. Gogineni and A. Nehorai, "Target estimation using sparse modeling for distributed MIMO radar," *IEEE Trans. Signal Process.*, vol. 59, no. 11, pp. 5315–5325, Nov. 2011.

- [27] A. P. Petropulu and H. V. Poor, "Measurement matrix design for compressive sensing based MIMO radar," *IEEE Trans. Signal Process.*, vol. 59, no. 11, pp. 5338–5352, Nov. 2011.
- [28] M. Rossi, A. Haimovich, and Y. Eldar, "Spatial compressive sensing for MIMO radar," *IEEE Trans. Signal Process.*, vol. 62, no. 2, pp. 419–430, Jan. 2014.
- [29] M. Bell, "Information theory and radar waveform design," *IEEE Trans. Inf. Theory*, vol. 39, no. 5, pp. 1578–1597, Sep. 1993.
- [30] J. Zhang, D. Zhu, and G. Zhang, "Adaptive compressed sensing radar oriented toward cognitive detection in dynamic sparse target scene," *IEEE Trans. Signal Process.*, vol. 60, no. 4, pp. 1718–1729, Apr. 2012.
- [31] J. Tropp, "Greed is good: Algorithmic results for sparse approximation," *IEEE Trans. Inf. Theory*, vol. 50, no. 10, pp. 2231–2242, Oct. 2004.
- [32] M. Elad, "Optimized projections for compressed sensing," *IEEE Trans. Signal Process.*, vol. 55, no. 12, pp. 5695–5702, Dec. 2007.
- [33] K. Ishibashi, K. Hatano, and M. Takeda, "Online learning of approximate maximum p-norm margin classifiers with biases," in *Proc. 21st Annu. COLT*, Helsinki, Finland, May 2008, pp. 154–161.
- [34] P. Stoica, J. Li, and X. Zhu, "Waveform synthesis for diversity-based transmit beam pattern design," *IEEE Trans. Signal Process.*, vol. 56, no. 6, pp. 2593–2598, Jun. 2008.
- [35] H. Li, C. Wang, K. Wang, Y. He, and X. Zhu, "High resolution range profile of compressive sensing radar with low computational complexity," *IET Radar, Sonar Navigat.*, vol. 9, no. 8, pp. 984–990, Oct. 2015.
- [36] Z. Liu, X. Wei, and X. Li, "Aliasing-free moving target detection in random pulse repetition interval radar based on compressed sensing," *IEEE Sensors J.*, vol. 13, no. 7, pp. 2523–2534, Jul. 2013.
- [37] Y. Chi and Y. Chen, "Compressive two-dimensional harmonic retrieval via atomic norm minimization," *IEEE Trans. Signal Process.*, vol. 63, no. 4, pp. 1030–1042, Feb. 2015.
- [38] M. Davenport and M. Wakin, "Analysis of orthogonal matching pursuit using the restricted isometry property," *IEEE Trans. Inf. Theory*, vol. 56, no. 9, pp. 4395–4401, Sep. 2010.
- [39] G. Galati and G. Pavan, "Waveforms design for modern and MIMO radar," in *Proc. IEEE EUROCON*, Zagreb, Croatia, Jul. 2013, pp. 508–513.
- [40] M. Herman and T. Strohmer, "High-resolution radar via compressed sensing," *IEEE Trans. Signal Process.*, vol. 57, no. 6, pp. 2275–2284, Jun. 2009.



**Lenan Wu** received the M.S. degree in electronics communication systems from Nanjing University of Aeronautics and Astronautics, Nanjing, China, in 1987 and the Ph.D. degree in signal and information processing from Southeast University, Nanjing, in 1997.

Since 1997, he has been with Southeast University, where he is currently a Professor and the Director of Multimedia Technical Research Institute. He is the author or coauthor of over 400 technical papers and 11 textbooks and is the holder of

20 Chinese patents and one international patent. His research interests include multimedia information systems and communication signal processing.



**Xianbin Wang** (S'98–M'99–SM'06) received the Ph.D. degree in electrical and computer engineering from the National University of Singapore, Singapore, in 2001.

From January 2001 to July 2002, he was a system designer with STMicroelectronics, where he was responsible for system design for DSL and Gigabit Ethernet chipsets. Between July 2002 and December 2007, he was with Communications Research Centre Canada as a Research Scientist/Senior Research Scientist. He is currently a Professor and the Canada

Research Chair with Western University, London, ON, Canada. He is the author of over 250 peer-reviewed journal and conference papers, in addition to 24 granted and pending patents and several standard contributions. His current research interests include fifth-generation networks, communications security, adaptive wireless systems, and locationing technologies.

Dr. Wang is an IEEE Distinguished Lecturer. He was involved in a number of IEEE conferences, including the IEEE Global Communications Conference; the IEEE International Conference on Communications; the IEEE Vehicular Technology Conference; the IEEE International Symposium on Personal, Indoor, and Mobile Radio Communications; the IEEE Wireless Communications and Networking Conference; and the IEEE Canadian Workshop on Information Technology, in different roles such as Symposium Chair, Tutorial Instructor, Track Chair, Session Chair, and Technical Program Committee Chair. He served as an Editor for IEEE TRANSACTIONS ON WIRELESS COMMUNICATIONS between 2007 and 2011. He currently serves as an Editor/Associate Editor for IEEE WIRELESS COMMUNICATIONS LETTERS, the IEEE TRANSACTIONS ON VEHICULAR TECHNOLOGY, and the IEEE TRANSACTIONS ON BROADCASTING. He has received many awards and recognitions, including the Canada Research Chair, the CRC Presidents Excellence Award, the Canadian Federal Government Public Service Award, the Ontario Early Researcher Award, and three IEEE Best Paper Awards.



**Peng Chen** (S'14) was born in Jiangsu, China, in 1989. He received the B.E. degree from the School of Information Science and Engineering from Southeast University, Nanjing, China, in 2011. He is currently working toward the Ph.D. degree with the School of Information Science and Engineering, Southeast University, under the supervision of Prof. L. Wu.

He is also a Visiting Ph.D. Student with the Department of Electrical Engineering, Columbia University, New York, NY, USA, under the supervision of Prof. X. Wang. His research interests include the

communication and radar signal processing, particularly with the radar system optimization.



**Chenhao Qi** (S'06–M'10–SM'15) received the B.S. and Ph.D. degrees in signal processing from Southeast University, Nanjing, China, in 2004 and 2010, respectively.

From 2008 to 2010, he visited the Department of Electrical Engineering, Columbia University, New York, NY, USA. Since 2010, he has been with the faculty of the School of Information Science and Engineering, Southeast University, where he is currently an Associate Professor. His research interests include sparse signal processing and wireless

communications.

Dr. Qi serves as a Reviewer and a Technical Program Committee Member for several international conferences.